

# Effect of nitrogen gas in the agglomeration and photoluminescence of Zn-ZnO nanowires after high-temperature annealing

R. López<sup>a,\*</sup>, G. García<sup>b</sup>, A. Coyopol<sup>c</sup>, T. Díaz<sup>b</sup>, and E. Rosendo<sup>b</sup>

<sup>a</sup>Laboratorio de Investigación y Desarrollo de Materiales Avanzados, Facultad de Química,

Universidad Autónoma del Estado de México, Toluca s/n, esq. Paseo Colón, Toluca, Estado de México, 50110, México.

<sup>b</sup>Centro de Investigaciones en Dispositivos Semiconductores-Instituto de Ciencias de la Universidad Autónoma de Puebla, 14 sur y Av. San Claudio, 72570, Puebla, México.

<sup>c</sup>Centro de Investigación en Materiales Avanzados unidad Monterrey, Parque de Investigación e Innovación Tecnológica, Km. 10 de la autopista Monterrey-Aeropuerto, Apodaca, NL, México.

Received 13 August 2015; accepted 13 October 2015

The effect of anti-agglomeration and enhanced photoluminescence after high-temperature annealing of Zn-ZnO nanowires in nitrogen atmosphere is reported. The Zn-ZnO nanowires were deposited by the hot filament chemical vapor deposition technique and subsequently annealed at 1100°C in oxygen or nitrogen atmospheres. It was found that under both annealing atmospheres, the structure of the nanowires was completely oxidized. Morphological studies suggest that annealing under oxygen-rich atmosphere, grain growth occurs, resulting in a continuous surface with a micrograin-shaped structure. However, it seems that nitrogen-rich annealing partially prevents complete agglomeration and longitudinal structures composed by nanometric grains were observed. Although photoluminescence properties of the annealed nanowires are improved in both annealing atmospheres, it was observed that the PL spectrum of nanowires annealed in nitrogen showed a stronger UV emission than that of the oxygen annealed nanowires.

*Keywords:* Nanowires; HFCVD; nitrogen annealing; ZnO.

PACS: 81.07.-b; 81.40.-z; 78.55.-m

## 1. Introduction

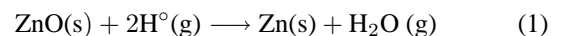
Nanostructured ZnO is a functional material with interesting physical properties for several applications such as dye-sensitized solar cells, excitonic lasing, biosensors, among others [1,2]. The availability of a variety of growth methods results in a large number of different ZnO morphologies and a wide range of nanostructure properties.

Thermal annealing is a process commonly used to reduce intrinsic defects, enlarging grain sizes, releasing accumulated strain energy, and thus improves crystallinity [3]. Additionally, optical properties of the thermal treated material are sensitive to the annealing atmosphere. For example, it has been reported that UV light emission is enhanced by annealing ZnO films in H<sub>2</sub> atmosphere [4], and that the optical properties of ZnO nanorods are improved by post-annealing treatment at 800°C [5]. Despite the benefits of thermal treatment process, the main disadvantage of annealing nanostructures is that grain-growth and agglomeration occurs, which results in formation of bigger particles or continuous structures that exhibit bulk properties [6]. Recently, some efforts have been made with the aim of prevent agglomeration of nanoparticles, subjecting them to smooth thermal annealing and using inert atmospheres [7,8]. In this sense, nitrogen gas is commonly employed in post-annealing treatments since it is fairly inert, in contrast with their oxygen and hydrogen counterparts. It has been also found that nitrogen influences the size of carbon nanotubes [9]. In the present work, the effect of anti-agglomeration in Zn-ZnO nanowires after annealing in nitrogen at 1100°C is studied. The nanowires were also

annealed in oxygen ambient to compare the effect of the gas atmosphere in the structural, morphological and photoluminescence properties.

## 2. Experimental details

Zn-ZnO nanowires were deposited on crystalline silicon wafers by the hot chemical vapor deposition (HFCVD) technique. ZnO pellets (0.23 g) were placed in a source holder, 2 mm under a tungsten filament. Hydrogen gas was flowed through a quartz tube at a rate of 100 standard cubic centimeters per minute (sccm). The process time and the substrate temperature were 100 s and 350°C, respectively. The main steps for formation of gas precursors are described as follows: first, the tungsten filament is heated up to about 2000°C by applying an AC voltage of 83.4 V. This temperature allows partial dissociation of molecular hydrogen into hydrogen atoms (H<sup>°</sup>), which are highly reactive and promote formation of a reducing gas atmosphere. The chemical reaction for decomposition of the ZnO pellet is proposed as follows:



After that, solid Zn is vaporized at 1200°C in the source holder. Thermal annealing was performed in a horizontal quartz tube at 1100°C for 2.5 hours at atmospheric pressure. During annealing, 99.998% purity oxygen or 99.998% purity nitrogen gases were introduced into the tube at a flow rate of 100 sccm. X-ray diffraction (XRD) patterns were measured

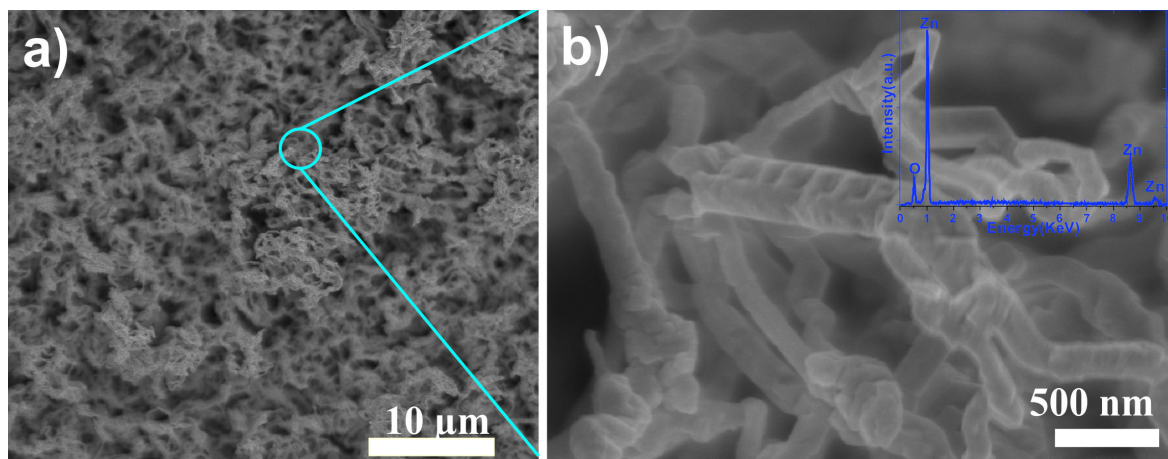


FIGURE 1. a) SEM image of Zn-ZnO nanowires deposited at 350°C by HFCVD, b) high-magnification image (the inset shows the corresponding EDS spectrum).

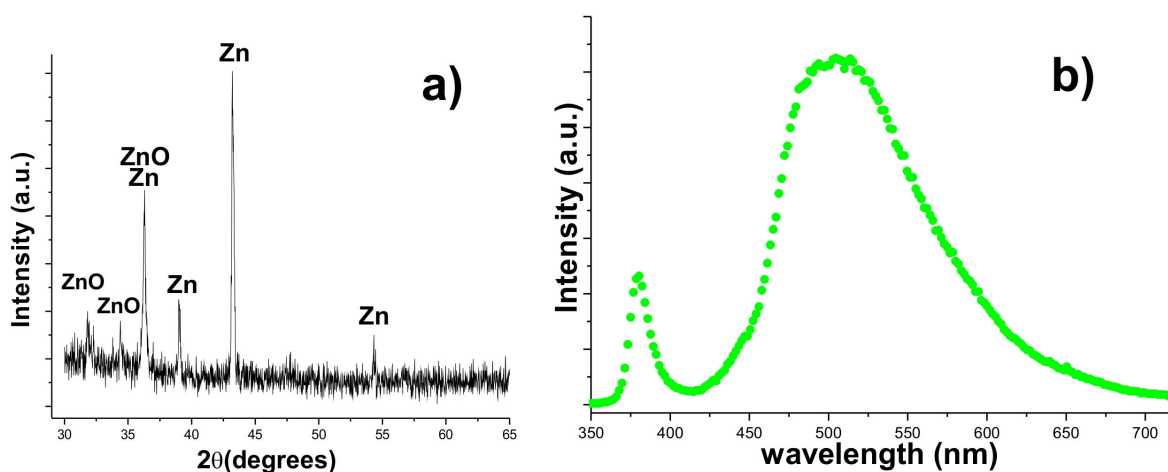


FIGURE 2. a) XRD pattern, and b) PL spectrum of the Zn-ZnO nanowires deposited at 350°C by HFCVD.

with a Bruker D8 Discover diffractometer using Cu  $K\alpha$  radiation (1.5418 Å). The morphology and elemental analysis by energy dispersive spectroscopy (EDS), were characterized using a scanning electron microscope (SEM) Phillips XL-30. Room-temperature photoluminescence (PL) measurements were performed using a 0.5 m long Science Tech double beam monochromator, a Hamamatsu photomultiplier tube (model 9040), and the 325 line of a He-Cd laser (Melles Griot) as excitation source.

### 3. Results and discussion

#### 3.1. As-deposited nanowires

Figure 1 shows SEM images of the products deposited by HFCVD at 350°C. Fig. 1a shows that the products exhibit a fibrous-like morphology with porous structure. High-magnification image in Fig. 1b reveals the presence of curved and entangled nanowires with irregular surfaces and diameters below 500 nm. The EDS analysis showed at the

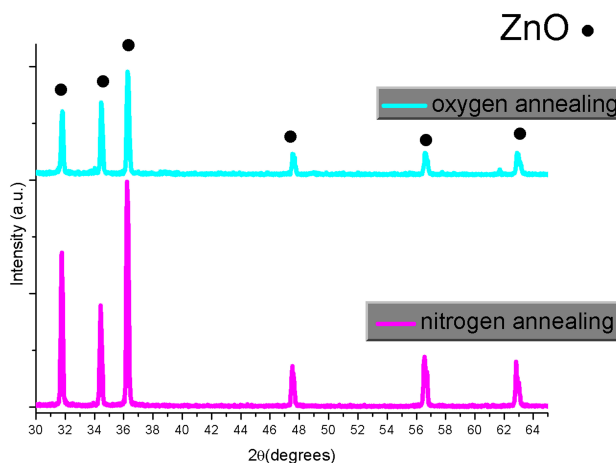


FIGURE 3. XRD patterns for Zn-ZnO nanowires annealed at 1100°C for 2.5 hours in oxygen or nitrogen atmospheres.

inset of Fig. 1b, indicates that the nanowires consist of Zn and oxygen only.

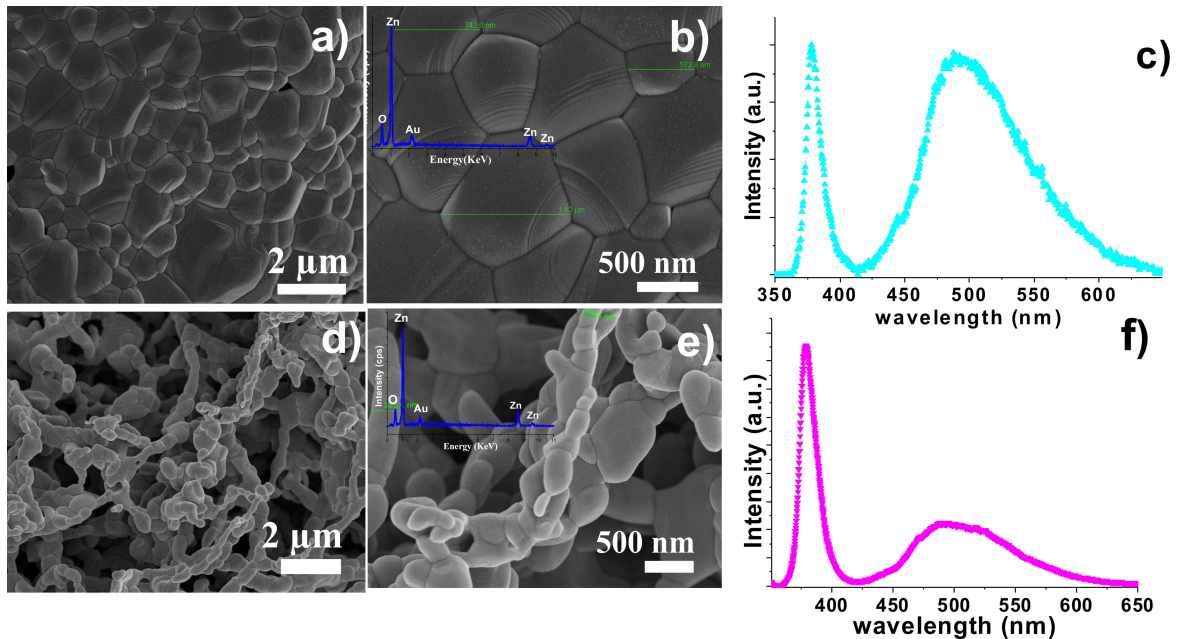


FIGURE 4. SEM images and PL spectra of the annealed Zn-ZnO nanowires: a)-c) SEM images and PL spectrum for oxygen annealed nanowires; d)-f) SEM images and PL spectrum of the nitrogen annealed nanowires. Insets in the high-magnification SEM images show the corresponding elemental analysis by EDS.

Figure 2 shows the XRD pattern and PL spectrum of nanowires deposited at  $350^{\circ}\text{C}$  by HFCVD. The peaks in the XRD pattern were indexed to crystalline Zn (JCPDS 00-004-0831) and ZnO (JCPDS 00-035-1451). The observation of only one kind of nanostructure in the SEM images and the results by XRD, suggest that Zn-ZnO nanowires were formed in the HFCVD experiments. The Zn peaks are stronger than the ZnO peaks, which could be evidence that the nanowires are mainly metallic particles. The PL spectrum shown in Fig. 2b includes a sharp but weak UV emission band and an intense broad visible emission band, centered at 380 and 505 nm, respectively. The UV emission band corresponds to the near band edge electron transition in ZnO, and the visible light emission centered in the green band is attributed to the non-stoichiometric composition of the ZnO, mainly originated for lack or excess of oxygen and Zn in ZnO, which is structurally represented by point defects such as oxygen vacancies ( $V_{\text{O}}$ ), interstitial oxygen, Zn vacancies and interstitial Zn (Zni) [10]. The strong visible emission may be related to a high quantity of surface  $V_{\text{O}}$  and Zni, usually formed in Zn-ZnO materials [11,12]. The mixture of Zn and ZnO in the structure of the nanowires suggests that vaporization of the ZnO pellet by the filament, and hence a physical vapor deposition mechanism can be ruled out. Thus, the growth of the nanowires seems to be governed by a vapor-solid mechanism. In thermal evaporation processes where experimental conditions such as atmospheric pressure and substrate temperatures around  $350^{\circ}\text{C}$  are employed, Zn nanowires have been collected on the inner wall of a quartz tube [13]. We have previously found that oxidation of Zn nanostructures starts in temperatures about  $314^{\circ}\text{C}$  [14]. Thus, it could be

assumed that surface of the nanowires deposited on the substrate surface heated at  $350^{\circ}\text{C}$  was oxidized by water vapor (as was proposed in Eq. 1).

### 3.2. Annealed nanowires

XRD patterns for nanowires annealed at  $1100^{\circ}\text{C}$  in oxygen or nitrogen atmosphere are shown in Fig. 3. As was expected, only peaks associated with the hexagonal wurtzite structure of ZnO are observed for nanowires annealed in flow of oxygen. For the Zn-ZnO nanowires annealed in nitrogen, a very similar oxidation behavior can be assumed since metal Zn peaks are not observed in their corresponding XRD pattern. This unexpected oxidation of the nanowires under flow of nitrogen could be caused by some impurities such as residual oxygen in the annealing environment [15], impurities of nitrogen used [16], or by oxygen atoms supplied by the quartz tube ( $\text{SiO}_2$ ) where annealing of the nanowires was performed [17]. The oxidation of Zn under nitrogen atmosphere has been observed to start even in temperatures below the melting point of Zn [14].

Figure 4 Shows SEM images and PL spectra for Zn-ZnO nanowires annealed in oxygen or nitrogen atmospheres at  $1100^{\circ}\text{C}$ . Fig. 4a shows the morphology for Zn-ZnO nanowires annealed in oxygen, which exhibits homogeneous surface with micrograin-like structure. Most of grains exhibit nanometric sizes (Fig. 4b). The formation of a continuous structure composed by grains with different sizes suggests that nucleation and growth occur throughout the high temperature annealing. EDS spectrum at the inset of Fig. 4b shows only Zn and oxygen peaks with the absence of any

other impurities such as carbon. The small Au peak is due to metallic gold that was sputter coated on the annealed Zn-ZnO nanowires to reduce electrical charging during SEM measurements. The PL spectrum for nanowires annealed in oxygen is shown in Fig. 4c. As can be seen, the UV emission was enhanced. The green emission intensity becomes lower because the Vo and the Zni are self-compensated under oxygen-rich condition. However, both emissions still have comparable intensities. This may be caused by the high number of grain boundaries in the microstructure of the nanowires annealed in oxygen ambient (as shown in Fig. 4a), which induces non-radiative recombination centers, resulting still in a low intensity UV emission. The morphology of the Zn-ZnO nanowires annealed in nitrogen is shown in Fig. 4d and 4e. The morphology seems to be similar to the as-deposited nanowires. It is difficult to understand the annealing process since high-temperature annealing at 1100°C should promote aggregation and coalescence of the nanowires, as was observed for the annealing in oxygen atmosphere. High-magnification image of the nanowires (Fig. 4e) shows that the structure of the nanowires is composed by connected particles or grains which have sizes mainly in the nanometric scale. The morphology of the grains for nitrogen annealed

nanowires is similar to that of the annealed in oxygen. However, under similar annealing conditions, it is suggested that nitrogen gas also prevents strong agglomeration of the ZnO grains and allows keeping the wire-shape. The corresponding EDS spectrum (inset of Fig. 4e), shows only Zn, oxygen and the Au peaks. Additionally, in the PL spectrum of the nitrogen annealed nanowires (Fig. 4f), it is observed that the UV emission was strongly enhanced and only a weak visible emission is present, which suggest that the nitrogen annealed nanowires have better optical properties than of the oxygen annealed nanowires.

#### 4. Conclusions

In summary, we have shown that nitrogen atmosphere partially prevents agglomeration of ZnO nanograins after high-temperature annealing and that the photoluminescence properties are enhanced by this post-treatment. It is clear that further studies are needed in order to clarify both assumptions. However, it is suggested that some nanostructures can be annealed at high-temperature, holding similar morphological and nanosized characteristics, which could be important in order to develop devices with nanometric properties.

- 
1. Xiao Wei Sun and Yi Yang, *ZnO nanostructures and Their Applications* CRC Press, Boca Raton, FL 33487-2742.
  2. A. Djuriscic, X. Chen, Y. Leung, A. Ching, *J Mater Chem* **22** (2012) 6526.
  3. B. Lin, Z. Fu, Y. Jia, *Appl Phys Lett* **79** (2001) 943.
  4. W. Shi, O. Agyeman, C. Xu, *J Appl Phys* **91** (2002) 5640.
  5. L. Quang, S. Chua, K. Loh, E. Fitzgerald, *J Cryst Growth* **287** (2006) 157.
  6. J. Cope, *Trans Faraday Soc* **67** (1961) 493.
  7. H. Chen *et al.*, *Chem Mater* **25** (2013) 1436.
  8. M. Moeinian, K. Akhbari, *Solid State Chem* **225** (2015) 459.
  9. R. Kurt, A. Karimi, *Chem Phys Chem* **2** (2001) 388.
  10. A. Khan, W. Jadwisieniczak, M. Kordesch, *Phys E* **33** (2006) 331.
  11. Y. Yan, P. Liu, M. Romero, M. Al-Jassim, *J Appl Phys* **93** (2003) 4807.
  12. X. Kong, Y. Ding, Z. Wang, *J Phys Chem B* **108** (2004) 570.
  13. S. Kar, T. Ghoshal, S. Chaudhuri, *Chem Phys Lett* **419** (2006) 174.
  14. P. Acuña, *et al.*, *AIP Advances* **5** (2015) 067109.
  15. J. Hu, Q. Li, X. Meng, C. Lee, S. Lee, *Chem Mater* **15** (2003) 305.
  16. W. Kan, C. Cao, G. Nabi, R. Yao, S. Bhatti, *J Alloy Compd* **506** (2010) 666.
  17. F. Zong, H. Ma, C. Hue, H. Zhuang, X. Zhang, H. Hiao, J. Ma, F. Ji, *Solid State Commun* **132** (2004) 521.